# Time-varying Output Group Formation and Tracking Control for Discrete-time Heterogeneous High-order Multi-agent System

**Nani Han, Keer Zhang**

*College of Electrical Engineering, Longdong University*
*(e-mail: hannani@yeah.net, gszhangkeer@163.com)*

**Abstract**: For the discrete-time heterogeneous high-order multi-agent system (MAS) with multiple leaders, the time-varying output group formation and tracking (TVOGFT) control problem is investigated in this paper. The followers are supposed to be partitioned into several groups, and are required to form different formations while track the average of leaders' outputs. Firstly, in order to estimate the leaders' states, the distributed observers considering the time-varying communication delay are proposed, and based on Lyapunov theory, the states of observers are proved to asymptotically reach the average of leaders' states. Then, the observer-based control protocols for followers of each group are designed, and the Algorithm regulating the control protocols is also offered. It is illustrated that the control protocols can make followers realize the TVOGFT by choosing appropriate formation functions and parameters. Finally, a MAS consisted of ten followers and three leaders is adopted to illustrates the effectiveness of the proposed protocols.

*Keywords*: Heterogeneous high-order multi-agent system; Discrete-time system; Time-varying output group formation; Tracking control; Communication delay.

## 1. INTRODUCTION

For the past few years, the distributed formation control of MAS has attracted extensive attention due to its widespread applications in many areas, such as target enclosing (Guo et al., 2010), cooperative competition (Zuo, 2020), load transportation (Maza et al., 2010) and so on. Compared with centralized coordination approaches, the distributed formation control has advantages in communications and computation performance.

As the basis of time-varying formation tracking (TVFT) control, there have been some researches about the time-varying formation (TVF) control for the homogeneous MAS, where all the agents have the identical dynamical model, such as second-order (Wang et al., 2020; Wang et al., 2020), high-order (Dong and Hu, 2016), fractional-order (Gong et al., 2020) and so on. The adaptive output-feedback approach (Wang et al., 2019; Wang et al., 2019) and event-triggered scheme (Li et al., 2019; Li et al., 2021) are usually adopted to solve the TVF problem.

In the TVFT control of homogeneous MAS, the followers are required to track leader's trajectories while form the desired formation (Hua et al., 2018). The influence factors, such as time-varying communication delay (Wang and Zhang, 2021), switching interaction topologies (Dong et al., 2019), input delay (Jiang et al., 2020), extern disturbance (Yu et al., 2020), and input saturation (Yu et al., 2020), can affect the performance of MAS and therefore need to be considered. The TVFT control with application to multiple aerial vehicles systems was studied in (Yu et al., 2021).

In the practical application, the agents usually have different structure and parameters, and the heterogeneous MAS is more suitable in this case. Since the agents in heterogeneous MAS have different dimensions, the outputs of agents are usually needed to achieve TVFT instead of states, namely time-varying output formation and tracking (TVOFT) problem. It is generally assumed that one leader (Hua et al., 2019) or convex combination of multiple leaders (Hua et al., 2019; Liu et al., 2021) is tracked in TVOFT. The distributed observer scheme (Hua et al., 2020; Qi et al., 2022) and adaptive control method (Duan et al., 2020) are often used to solve the TVOFT problem. When the multiple leaders communicate with each other, then it becomes formation-containment problem (Zuo et al., 2019; Gao et al., 2021).

In the aforementioned works, whether the TVF, TVFT, or formation-containment problem, all agents are controlled to form only one desired formation. However, when agents are required to perform different tasks simultaneously, they need to be divided into several groups and form different formations (Dong et al., 2017). It needs to be noticed that TVOGFT is not simple superposition of TVOFT of different groups due to their communications between groups. In (Li et al., 2018; Zhou et al., 2021), the leaders were assigned to each group of followers, and the followers were required to track the leader which belonged to the same group. By contrast, the followers were controlled to track the average of leaders' states in (Han et al., 2020). The application of TVOGFT to air ground cooperative control was investigated in (Tian et al., 2020).

In the application of MAS, communication delay is often considered, which will not only affect the performance of the system, even destroy the stability of the system (Zhang et al., 2008; Chen and Li, 2009; Qaisar et al., 2020). In this paper, for the discrete-time heterogeneous MAS, the TVOGFT problem with time-varying delay under directed topology is studied. Firstly, the distributed observers are presented and the effectiveness is proved by using Lyapunov theory. Then the observer-based TVOGFT protocols are constructed. It is proved that the protocols can make the followers achieve TVOGFT when formation feasibility conditions are satisfied. In additional, an algorithm to construct the designed protocols is also presented.

Compared with the existing researches, the contributions of this paper are summarized as follows. First, the discrete-time heterogeneous MAS is considered. The dynamics in (Han et al., 2020; Li et al., 2018; Dong et al., 2017) were described as second-order and high-order homogeneous MASs. The dynamics in (Tian et al., 2020; Zhou et al., 2021) were assumed to be continuous. In (Qi et al., 2022), the system was assumed to be discrete-time and heterogeneous, but the followers finally formed only one desired formation. Second, we assume that there exist multiple leaders. In (Zhou et al., 2021), the followers were required to follow the only one leader which belonged to the same group with followers. The multiple leaders were considered in (Hua et al., 2019; Liu et al., 2021; Hua et al., 2020; Qi et al., 2022), but the followers were not divided into different groups. Third, the discrete-time communication delay is taken into account which is not considered in (Li et al., 2018; Dong et al., 2017; Tian et al., 2020).

Next, this paper is arranged as follows. The basic graph theory and system description are presented in section 2. Section 3 is the TVOGFT research results, including observers, TVOGFT protocols and algorithm. The simulation results are given in section 4. Finally, section 5 is the conclusion summarizing the whole work.

In this paper, $\boldsymbol{1}_{n_{\bar{i}}\times(N-M)}$ and $\boldsymbol{1}_{n_{\bar{i}}}$ represent $n_{\bar{i}}\times(N-M)$ -dimensional matrix and $n_{\bar{i}}$ -dimensional column vector with all elements 1 respectively. $\boldsymbol{I}$ denotes an identity matrix with appreciate dimension, and $\otimes$ is defined as the Kronecker product. $\boldsymbol{\Lambda}_S = diag\{\boldsymbol{S},\boldsymbol{S}\}$ is a block-diagonal matrix with diagonal values $\boldsymbol{S}$ . Matrix $\boldsymbol{\gamma}_{\lambda_i} = \begin{bmatrix} \mathrm{Re}(\lambda_i) & -\mathrm{Im}(\lambda_i) \\ \mathrm{Im}(\lambda_i) & \mathrm{Re}(\lambda_i) \end{bmatrix}$, where $\mathrm{Re}(\lambda_i)$ and $\mathrm{Im}(\lambda_i)$ are the real and imaginary parts of complex number $\lambda_i$ , respectively. .

## 2. GRAPH THEORY AND PROBLEM DESCRIPTION

### *2.1 Graph Theory*

The interconnection of a MAS consisted of $N$ agents can be described by graph $G=\{V,E,\boldsymbol{W}\}$ , in which $V=\{v_1,v_2,\cdots,v_N\}$ is the node set, $E=\{e_{ij}=(v_i,v_j)\}$ denotes the set of edges. $\boldsymbol{W}=[w_{ij}]\in\mathbb{R}^{N\times N}$ is the weighted adjacent matrix, and $w_{ij}>0$ if $e_{ij}\in E$ , or $w_{ij}=0$ , $w_{ii}=0$ for all $i$ . When there exists information flow form node $j$ to node $i$ , then node $j$ is a neighbor of $i$ , and all neighbors of $i$ is denoted by $N_i$. The asymmetric Laplacian matrix is denoted by $\boldsymbol{L}=[l_{ij}]_{N\times N}$ , where $l_{ii}=\sum_{j=1,j\neq i}^{N} w_{ij}$ and $l_{ij}=-w_{ij}$ for $i\neq j$ . (Godsil and Royle, 2001).

### *2.2 Problem Description*

Considering a heterogeneous MAS consisted of $N$ agents, in which $M$ agents are defined as followers, the rest $N-M$ agents are leaders. The dynamics of followers are described as

$$\begin{cases} \boldsymbol{x}_i(k+1)=\boldsymbol{A}_i\boldsymbol{x}_i(k)+\boldsymbol{B}_i\boldsymbol{u}_i(k) \\ \boldsymbol{y}_i(k)=\boldsymbol{C}_i\boldsymbol{x}_i(k) \end{cases}, i=1,2,\cdots,M \tag{1}$$

where $\boldsymbol{x}_i(k)\in\mathbb{R}^{n_i}$ , $\boldsymbol{u}_i(k)\in\mathbb{R}^{m_i}$ , $\boldsymbol{y}_i(k)\in\mathbb{R}^{p}$ are the state, control input and output of followers $i$ at time instant $k$ , respectively. $\boldsymbol{A}_i\in\mathbb{R}^{n_i\times n_i}$ , $\boldsymbol{B}_i\in\mathbb{R}^{n_i\times m_i}$ , $\boldsymbol{C}_i\in\mathbb{R}^{p\times n_i}$ are known constant matrices with $rank(\boldsymbol{B}_i)=m_i$ . Assume that the pairs $(\boldsymbol{A}_i,\boldsymbol{B}_i)$ are stabilizable and the pairs $(\boldsymbol{C}_i,\boldsymbol{A}_i)$ are detectable.

The leaders are described as

$$\begin{cases} \boldsymbol{x}_j(k+1)=\boldsymbol{S}\boldsymbol{x}_j(k) \\ \boldsymbol{y}_j(k)=\boldsymbol{U}\boldsymbol{x}_j(k) \end{cases}, j=M+1,M+2,\cdots,N \tag{2}$$

where $\boldsymbol{x}_j(k)\in\mathbb{R}^{q}$ , $\boldsymbol{y}_j(k)\in\mathbb{R}^{p}$ are the state and output of leader $j$ at time instant $k$ , respectively. $\boldsymbol{S}\in\mathbb{R}^{q\times q},\boldsymbol{U}\in\mathbb{R}^{p\times q}$ are constant matrices. The pair $(\boldsymbol{U},\boldsymbol{S})$ is observable. And the eigenvalues of the matrix $\boldsymbol{S}$ are all outside the unit circle.

*Assumption 1*: The following regulation equations

$$\begin{cases} \boldsymbol{E}_i\boldsymbol{S}=\boldsymbol{A}_i\boldsymbol{E}_i+\boldsymbol{B}_i\boldsymbol{F}_i \\ \boldsymbol{0}=\boldsymbol{C}_i\boldsymbol{E}_i-\boldsymbol{U} \end{cases} \tag{3}$$

have solution pairs $(\boldsymbol{E}_i,\boldsymbol{F}_i), i=1,2,\cdots,M$ .

To achieve TVOGFT control, the $M$ followers are supposed to be divided into $g\in\mathbb{N}(g\geq 1)$ groups and the node set of $g$ groups is denoted by $\{V_1,V_2,\cdots,V_g\}$ which satisfies $V_k\neq\varnothing(k=1,2,\cdots,g)$ , $\bigcup_{k=1}^{g}V_k=V$ and $V_k\bigcap V_l=\varnothing$ $(k,l\in\{1,2,\cdots,g\},k\neq l)$ . Let $\bar{i}$ be the index of group that agent $i$ belongs to. The number of followers in each group $\bar{i}\,(\bar{i}=1,2,\cdots,g)$ is denoted by $n_{\bar{i}}$ . The node set of each group is represented by $V_{\bar{i}}=\{\Xi_{\bar{i}}+1,\Xi_{\bar{i}}+2,\cdots,\Xi_{\bar{i}}+n_{\bar{i}}\}$ with $\Xi_{\bar{i}}=\sum_{k=0}^{\bar{i}-1}n_k$ , $n_0=0$ .

*Assumption 2*: $\{V_1,V_2,\cdots,V_g\}$ is an acyclic division of the node set $V$ .

*Assumption 3*: In each group, there exists at least one follower which can obtain the information of all leaders, namely well-informed agent, and the rest are uninformed agents which can’t receive any information from leaders. For each uninformed agent, there exists at least one well-informed agent in the same group which has a directed path to it.

Base on *Assumption 2* and *Assumption 3*, the Laplacian matrix $\boldsymbol{L}$ has the following form

$$\boldsymbol{L}=\begin{bmatrix}\boldsymbol{L}_1 & \boldsymbol{L}_2\\ \boldsymbol{0} & \boldsymbol{0}\end{bmatrix} \tag{4}$$

where, $\boldsymbol{L}_1 \in \mathbb{R}^{M\times M}$, $\boldsymbol{L}_2 \in \mathbb{R}^{M\times(N-M)}$.

$$\boldsymbol{L}_1=\begin{bmatrix}\boldsymbol{L}_{11} & \boldsymbol{0} & \cdots & \boldsymbol{0}\\ \boldsymbol{L}_{21} & \boldsymbol{L}_{22} & \cdots & \boldsymbol{0}\\ \vdots & \vdots & \vdots & \vdots\\ \boldsymbol{L}_{g1} & \boldsymbol{L}_{g2} & \cdots & \boldsymbol{L}_{gg}\end{bmatrix} \tag{5}$$

*Assumption 4:* Each row sum of $\boldsymbol{L}_{\bar{i}\bar{j}}(\bar{i}>\bar{j})$ equals to 0.

*Remark 1*: $\boldsymbol{L}_{\bar{i}\bar{i}}(\bar{i}=1,2,\cdots,g)$ is the interaction topology of the followers in group $\bar{i}$, and $\boldsymbol{L}_{\bar{i}\bar{j}}(\bar{i}>\bar{j})$ describes the interaction between the group $\bar{i}$ and $\bar{j}$. When agent $i$ and agent $j$ are in the same group, then $w_{ij}=1$ if $(v_j,v_i)\in E$, otherwise $w_{ij}=0$. When agent $i$ and agent $j$ are in the different groups $\bar{i}$ and $\bar{j}(\bar{i}>\bar{j})$, $w_{ij}=2$ if $(v_j,v_i)\in E$ and group $\bar{i}$ and $\bar{j}$ interact cooperatively, if $(v_j,v_i)\in E$ and group $\bar{i}$ and $\bar{j}$ interact competitively, $w_{ij}=-2$, otherwise $w_{ij}=0$.

*Lemma 1* (Li et al., 2015): When *Assumption 3* holds, all the eigenvalues of matrix $\boldsymbol{L}_1$ have positive real parts.

*Lemma 2* (Hu et al., 2019): If *Assumption 3* and *Assumption 4* hold simultaneously, then $-\boldsymbol{L}_1^{-1}\boldsymbol{L}_2$ has the following form

$$-\boldsymbol{L}_1^{-1}\boldsymbol{L}_2=\begin{bmatrix}\boldsymbol{\alpha}_1^{\mathrm{T}} & \boldsymbol{\alpha}_2^{\mathrm{T}} & \cdots & \boldsymbol{\alpha}_g^{\mathrm{T}}\end{bmatrix}^{\mathrm{T}} \tag{6}$$

where $\boldsymbol{\alpha}_{\bar{i}}=\boldsymbol{1}_{n_{\bar{i}}\times(N-M)}/N-M$.

Let $\boldsymbol{h}_i^{\bar{i}}(k)\in\mathbb{R}^q(\bar{i}=1,2,\cdots,g)$ denote the desired state formation function of agent $i$ in group $\bar{i}(\bar{i}=1,2,\cdots,g)$, and the corresponding output formation is $\boldsymbol{h}_{oi}^{\bar{i}}(k)=\boldsymbol{U}\boldsymbol{h}_i^{\bar{i}}(k)(\bar{i}=1,2,\cdots,g)$.

Denote $\boldsymbol{h}_o^{\bar{i}}(k)=\begin{bmatrix}\boldsymbol{h}_{o(\Xi_{\bar{i}}+1)}^{\mathrm{T}},\boldsymbol{h}_{o(\Xi_{\bar{i}}+2)}^{\mathrm{T}},\cdots,\boldsymbol{h}_{o(\Xi_{\bar{i}}+n_{\bar{i}})}^{\mathrm{T}}\end{bmatrix}^{\mathrm{T}}$, $\boldsymbol{y}^{\bar{i}}(k)=\begin{bmatrix}\boldsymbol{y}_{\Xi_{\bar{i}}+1}^{\mathrm{T}},\boldsymbol{y}_{\Xi_{\bar{i}}+2}^{\mathrm{T}},\cdots,\boldsymbol{y}_{\Xi_{\bar{i}}+n_{\bar{i}}}^{\mathrm{T}}\end{bmatrix}^{\mathrm{T}}$ for the group $\bar{i}(\bar{i}=1,2,\cdots,g)$.

*Definition 1*: For any bounded initial states and any group $\bar{i}(\bar{i}=1,2,\cdots,g)$, the TVOGFT control is realized if

$$\lim_{k\to\infty}\left(\boldsymbol{y}^{\bar{i}}(k)-\boldsymbol{h}_o^{\bar{i}}(k)-\frac{\boldsymbol{1}_{n_{\bar{i}}}}{N-M}\otimes\sum_{j=M+1}^{N}\boldsymbol{y}_j(k)\right)=\boldsymbol{0} \tag{7}$$

*Remark 2*: In *Definition 1*, $\left(\boldsymbol{1}_{n_{\bar{i}}}/(N-M)\right)\otimes\sum_{j=M+1}^{N}\boldsymbol{y}_j(k)$ is the average of leaders' outputs, which is a special case of convex combination of leaders' outputs and can be regarded as the formation reference function.

## 3. MAIN RESULTS

In this part, the distributed observers using the outputs of neighbors are designed for each follower firstly, and the effectiveness is illustrated by using Lyapunov theory. Then, the observer-based control protocols are presented. And the algorithm regulating the steps to construct the protocols is also given.

In order to estimate the average of leaders' states, the distributed observers are designed as follows

$$\begin{aligned}\hat{\boldsymbol{\xi}}_i^{\bar{i}}(k+1)&=\boldsymbol{S}\hat{\boldsymbol{\xi}}_i^{\bar{i}}(k)-\boldsymbol{K}_1\sum_{j\in N_i}^{c=\bar{i}}w_{ij}(\hat{\boldsymbol{y}}_i^{\bar{i}}(k-\tau_k)-\hat{\boldsymbol{y}}_j^{c}(k-\tau_k))-\\ &\boldsymbol{K}_1\sum_{j\in N_i}^{c\neq\bar{i}}w_{ij}(\hat{\boldsymbol{y}}_i^{\bar{i}}(k-\tau_k)-\hat{\boldsymbol{y}}_j^{c}(k-\tau_k))-\\ &\boldsymbol{K}_1\sum_{j=M+1}^{N}w_{ij}(\hat{\boldsymbol{y}}_i^{\bar{i}}(k-\tau_k)-\boldsymbol{y}_j(k-\tau_k)),\bar{i}=1,2,\cdots,g\end{aligned} \tag{8}$$

where $\hat{\boldsymbol{\xi}}_i^{\bar{i}}(k)\in\mathbb{R}^q$ is the observer state of agent $i(i=1,2,\cdots,M)$ in group $\bar{i}(\bar{i}=1,2,\cdots,g)$, $\hat{\boldsymbol{y}}_i^{\bar{i}}(k)=\boldsymbol{U}\hat{\boldsymbol{\xi}}_i^{\bar{i}}(k)$, $\boldsymbol{y}_j(k)=\boldsymbol{U}\boldsymbol{x}_j(k)$, $\boldsymbol{K}_1\in\mathbb{R}^{q\times p}$ is the constant gain matrix. $\tau_k$ is the time-varying communication delay satisfying

$$\tau_m\le\tau_k\le\tau_M \tag{9}$$

with $\tau_m$ and $\tau_M$ being known positive integers.

Denote $\hat{\boldsymbol{\xi}}^{\bar{i}}(k)=\begin{bmatrix}\hat{\boldsymbol{\xi}}_{\Xi_{\bar{i}}+1}^{\bar{i}\mathrm{T}}(k),\hat{\boldsymbol{\xi}}_{\Xi_{\bar{i}}+2}^{\bar{i}\mathrm{T}}(k),\cdots,\hat{\boldsymbol{\xi}}_{\Xi_{\bar{i}}+n_{\bar{i}}}^{\bar{i}\mathrm{T}}(k)\end{bmatrix}^{\mathrm{T}}$, $\hat{\xi}(k)=\begin{bmatrix}\hat{\boldsymbol{\xi}}^{1\mathrm{T}}(k),\hat{\boldsymbol{\xi}}^{2\mathrm{T}}(k),\cdots,\hat{\boldsymbol{\xi}}^{g\mathrm{T}}(k)\end{bmatrix}^{\mathrm{T}}$, $\boldsymbol{x}_E(k)=\begin{bmatrix}\boldsymbol{x}_{M+1}^{\mathrm{T}}(k),\boldsymbol{x}_{M+2}^{\mathrm{T}}(k),\cdots,\boldsymbol{x}_N^{\mathrm{T}}(k)\end{bmatrix}^{\mathrm{T}}$, then the distributed observers (8) can be rewritten as

$$\begin{aligned}\hat{\xi}(k+1)&=(\boldsymbol{I}_M\otimes\boldsymbol{S})\hat{\xi}(k)-(\boldsymbol{L}_1\otimes\boldsymbol{K}_1\boldsymbol{U})\hat{\xi}(k-\tau_k)-\\ &(\boldsymbol{L}_2\otimes\boldsymbol{K}_1\boldsymbol{U})\boldsymbol{x}_E(k-\tau_k)\end{aligned} \tag{10}$$

*Lemma 3* (Mahnoud, 2004): For any real vectors $\boldsymbol{a}$, $\boldsymbol{b}$ and any matrix $\boldsymbol{Q}>0$ with appropriate dimension, then

$$\pm2\boldsymbol{a}^{\mathrm{T}}\boldsymbol{b}\le\boldsymbol{a}^{\mathrm{T}}\boldsymbol{Q}\boldsymbol{a}+\boldsymbol{b}^{\mathrm{T}}\boldsymbol{Q}^{-1}\boldsymbol{b} \tag{11}$$

When *Assumption 3* holds, there exits nonsingular matrix $\boldsymbol{Z}^{-1}$ satisfying $\boldsymbol{Z}^{-1}\boldsymbol{L}_1\boldsymbol{Z}=\boldsymbol{J}$, where $\boldsymbol{J}$ is the Jordan form of $\boldsymbol{L}_1$. Denote $\lambda_i(i=1,2,\cdots,M)$ is the eigenvalues of $\boldsymbol{L}_1$, and define $\bar{\lambda}_{1,2}=\min\{\mathrm{Re}(\lambda_i)\}\pm j\bar{\mu}$, $\bar{\lambda}_{3,4}=\max\{\mathrm{Re}(\lambda_i)\}\pm j\bar{\mu}$, $\bar{\mu}=\max\{\mathrm{Im}(\lambda_i)\}$. Then *Lemma 4* is given as following.

*Lemma 4* (Xi et al., 2001): Assume $\boldsymbol{\Phi}_0,\boldsymbol{\Phi}_1,\boldsymbol{\Phi}_2$ are real symmetric matrices, if $\boldsymbol{\Phi}_0+\mathrm{Re}(\bar{\lambda}_i)\boldsymbol{\Phi}_1+\mathrm{Im}(\bar{\lambda}_i)\boldsymbol{\Phi}_2<0$ $(i=1,2,3,4)$, then $\boldsymbol{\Phi}_0+\mathrm{Re}(\lambda_i)\boldsymbol{\Phi}_1+\mathrm{Im}(\lambda_i)\boldsymbol{\Phi}_2<0$ $(i=1,2,\cdots,M)$。

*Theorem 1*: Suppose *Assumption 3* and *Assumption 4* hold, the distributed observers (8) with time-varying communication delay will converge to the average of leaders' states, that is

$$\lim_{k\to\infty}\left(\hat{\boldsymbol{\xi}}^{\bar{i}}(k)-\left(\boldsymbol{1}_{n_{\bar{i}}}/(N-M)\right)\otimes\sum\nolimits_{j=M+1}^{N}\boldsymbol{x}_j(k)\right)=\boldsymbol{0},$$
$$\bar{i}=1,2,\cdots,g. \tag{12}$$

if there exist positive definite symmetric matrices $\boldsymbol{P},\boldsymbol{Q}_1,\boldsymbol{Q}_2,\boldsymbol{Q}_3,\boldsymbol{R},\boldsymbol{\Gamma}$ and matrices $\boldsymbol{D}_1,\boldsymbol{D}_2,\boldsymbol{T}_1,\boldsymbol{T}_2,\boldsymbol{\Psi}_1,\boldsymbol{\Psi}_2$ satisfy

$$\begin{bmatrix}\boldsymbol{\Theta}_{11} & \boldsymbol{\Theta}_{12} & \boldsymbol{T}_1 & \boldsymbol{\Theta}_{14} & \boldsymbol{\Theta}_{15} & \boldsymbol{\Theta}_{16} & \boldsymbol{\Theta}_{17} & \boldsymbol{\Theta}_{18} & \boldsymbol{\Theta}_{19} & \boldsymbol{\Theta}_{110}\\ * & \boldsymbol{\Theta}_{22} & \boldsymbol{T}_2 & \boldsymbol{\Theta}_{24} & \boldsymbol{\Theta}_{25} & \boldsymbol{\Theta}_{26} & \boldsymbol{\Theta}_{27} & \boldsymbol{\Theta}_{28} & \boldsymbol{\Theta}_{29} & \boldsymbol{\Theta}_{210}\\ * & * & \boldsymbol{\Theta}_{33} & \boldsymbol{0} & \boldsymbol{0} & \boldsymbol{0} & \boldsymbol{0} & \boldsymbol{0} & \boldsymbol{0} & \boldsymbol{0}\\ * & * & * & \boldsymbol{\Theta}_{44} & \boldsymbol{0} & \boldsymbol{0} & \boldsymbol{0} & \boldsymbol{0} & \boldsymbol{0} & \boldsymbol{0}\\ * & * & * & * & \boldsymbol{\Theta}_{55} & \boldsymbol{0} & \boldsymbol{0} & \boldsymbol{0} & \boldsymbol{0} & \boldsymbol{0}\\ * & * & * & * & * & \boldsymbol{\Theta}_{66} & \boldsymbol{0} & \boldsymbol{0} & \boldsymbol{0} & \boldsymbol{0}\\ * & * & * & * & * & * & \boldsymbol{\Theta}_{77} & \boldsymbol{0} & \boldsymbol{0} & \boldsymbol{0}\\ * & * & * & * & * & * & * & -\boldsymbol{P} & \boldsymbol{0} & \boldsymbol{0}\\ * & * & * & * & * & * & * & * & -\boldsymbol{R} & \boldsymbol{0}\\ * & * & * & * & * & * & * & * & * & -\boldsymbol{\Gamma}\end{bmatrix}<0$$
$$(i=1,2,3,4) \tag{13}$$

where $\boldsymbol{\Theta}_{11}=-\boldsymbol{P}+(\rho+1)\boldsymbol{Q}_1+\boldsymbol{Q}_2+\boldsymbol{Q}_3+\boldsymbol{\Psi}_1+\boldsymbol{\Psi}_1^{\mathrm{T}}$, $\boldsymbol{\Theta}_{12}=\boldsymbol{\Psi}_2^{\mathrm{T}}-\boldsymbol{\Psi}_1-\boldsymbol{T}_1+\boldsymbol{D}_1$, $\boldsymbol{\Theta}_{14}=-\boldsymbol{D}_1$, $\boldsymbol{\Theta}_{15}=\sqrt{\rho}\boldsymbol{D}_1$, $\boldsymbol{\Theta}_{16}=\sqrt{\rho}\boldsymbol{T}_1$, $\boldsymbol{\Theta}_{17}=\sqrt{\tau_M}\boldsymbol{\Psi}_1$, $\boldsymbol{\Theta}_{18}=\boldsymbol{\Lambda}_S^{\mathrm{T}}\boldsymbol{P}$, $\boldsymbol{\Theta}_{19}=\sqrt{\rho}\left(\boldsymbol{\Lambda}_S-\boldsymbol{I}\right)^{\mathrm{T}}\boldsymbol{R}$, $\boldsymbol{\Theta}_{110}=\sqrt{\tau_M}\left(\boldsymbol{\Lambda}_S-\boldsymbol{I}\right)^{\mathrm{T}}\boldsymbol{\Gamma}$, $\boldsymbol{\Theta}_{22}=-\boldsymbol{Q}_1-\boldsymbol{\Psi}_2-\boldsymbol{\Psi}_2^{\mathrm{T}}-\boldsymbol{T}_2-\boldsymbol{T}_2^{\mathrm{T}}+\boldsymbol{D}_2+\boldsymbol{D}_2^{\mathrm{T}}$, $\boldsymbol{\Theta}_{24}=-\boldsymbol{D}_2$, $\boldsymbol{\Theta}_{25}=\sqrt{\rho}\boldsymbol{D}_2$, $\boldsymbol{\Theta}_{26}=\sqrt{\rho}\boldsymbol{T}_2$, $\boldsymbol{\Theta}_{27}=\sqrt{\tau_M}\boldsymbol{\Psi}_2$, $\boldsymbol{\Theta}_{28}=-(\gamma_{\bar{\lambda}_i}\boldsymbol{\Lambda}_{K_1U})^{\mathrm{T}}\boldsymbol{P}$, $\boldsymbol{\Theta}_{29}=-\sqrt{\rho}(\gamma_{\bar{\lambda}_i}\boldsymbol{\Lambda}_{K_1U})^{\mathrm{T}}\boldsymbol{R}$, $\boldsymbol{\Theta}_{210}=-\sqrt{\tau_M}(\gamma_{\bar{\lambda}_i}\boldsymbol{\Lambda}_{K_1U})^{\mathrm{T}}\boldsymbol{\Gamma}$, $\boldsymbol{\Theta}_{33}=-\boldsymbol{Q}_2$, $\boldsymbol{\Theta}_{44}=-\boldsymbol{Q}_3$, $\boldsymbol{\Theta}_{55}=-\left(\boldsymbol{R}+\boldsymbol{\Gamma}\right)$, $\boldsymbol{\Theta}_{66}=-\boldsymbol{R}$, $\boldsymbol{\Theta}_{77}=-\boldsymbol{\Gamma}$, $\rho=\tau_M-\tau_m$.

*Proof*: Let $\tilde{\boldsymbol{\xi}}(k)=\hat{\boldsymbol{\xi}}(k)-\left(-\boldsymbol{L}_1^{-1}\boldsymbol{L}_2\otimes\boldsymbol{I}_q\right)\boldsymbol{x}_E(k)$, then

$$\tilde{\boldsymbol{\xi}}(k+1)=\left(\boldsymbol{I}_M\otimes\boldsymbol{S}\right)\tilde{\boldsymbol{\xi}}(k)-\left(\boldsymbol{L}_1\otimes\boldsymbol{K}_1\boldsymbol{U}\right)\tilde{\boldsymbol{\xi}}(k-\tau_k) \tag{14}$$

Denote $\boldsymbol{\eta}(k)=\left(\boldsymbol{Z}^{-1}\otimes\boldsymbol{I}_q\right)\tilde{\boldsymbol{\xi}}(k)$, then

$$\boldsymbol{\eta}(k+1)=\left(\boldsymbol{I}_M\otimes\boldsymbol{S}\right)\boldsymbol{\eta}(k)-\left(\boldsymbol{J}\otimes\boldsymbol{K}_1\boldsymbol{U}\right)\boldsymbol{\eta}(k-\tau_k) \tag{15}$$

Considering the following systems' stabilities

$$\boldsymbol{\eta}_i(k+1)=\boldsymbol{S}\boldsymbol{\eta}_i(k)-\lambda_i\boldsymbol{K}_1\boldsymbol{U}\boldsymbol{\eta}_i(k-\tau_k),i=1,2,\cdots,M \tag{16}$$

Let $\tilde{\boldsymbol{\eta}}_i(k)=\left[\mathrm{Re}^{\mathrm{T}}\left(\boldsymbol{\eta}_i(k)\right)\quad \mathrm{Im}^{\mathrm{T}}\left(\boldsymbol{\eta}_i(k)\right)\right]^{\mathrm{T}}$, then

$$\tilde{\boldsymbol{\eta}}_i(k+1)=\boldsymbol{\Lambda}_S\tilde{\boldsymbol{\eta}}_i(k)-\gamma_{\lambda_i}\boldsymbol{\Lambda}_{K_1U}\tilde{\boldsymbol{\eta}}_i(k-\tau_k),i=1,2,\cdots,M \tag{17}$$

Denote $\boldsymbol{\upsilon}_i(k)=\tilde{\boldsymbol{\eta}}_i(k+1)-\tilde{\boldsymbol{\eta}}_i(k)(i=1,2,\cdots,M)$, and choose the following Lyapunov functional candidates

$$V_i(k)=\sum_{j=1}^{6}V_{ij}(k),i=1,2,\cdots,M \tag{18}$$

where,

$$V_{i1}(k)=\tilde{\boldsymbol{\eta}}_i^{\mathrm{T}}(k)\boldsymbol{P}\tilde{\boldsymbol{\eta}}_i(k),$$
$$V_{i2}(k)=\sum_{l=k-\tau_k}^{k-1}\tilde{\boldsymbol{\eta}}_i^{\mathrm{T}}(l)\boldsymbol{Q}_1\tilde{\boldsymbol{\eta}}_i(l),$$
$$V_{i3}(k)=\sum_{l=k-\tau_m}^{k-1}\tilde{\boldsymbol{\eta}}_i^{\mathrm{T}}(l)\boldsymbol{Q}_2\tilde{\boldsymbol{\eta}}_i(l)+\sum_{l=k-\tau_M}^{k-1}\tilde{\boldsymbol{\eta}}_i^{\mathrm{T}}(l)\boldsymbol{Q}_3\tilde{\boldsymbol{\eta}}_i(l),$$
$$V_{i4}(k)=\sum_{j=-\tau_M+1}^{-\tau_m}\sum_{l=k+j}^{k-1}\tilde{\boldsymbol{\eta}}_i^{\mathrm{T}}(l)\boldsymbol{Q}_1\tilde{\boldsymbol{\eta}}_i(l),$$
$$V_{i5}(k)=\sum_{j=-\tau_M}^{-\tau_m-1}\sum_{l=k+j}^{k-1}\boldsymbol{\upsilon}_i^{\mathrm{T}}(l)\boldsymbol{R}\boldsymbol{\upsilon}_i(l),$$
$$V_{i6}(k)=\sum_{j=-\tau_M}^{-1}\sum_{l=k+j}^{k-1}\boldsymbol{\upsilon}_i^{\mathrm{T}}(l)\boldsymbol{\Gamma}\boldsymbol{\upsilon}_i(l).$$

Then, along the solution of (17) there exist

$$\Delta V_{i1}(k)=\tilde{\boldsymbol{\eta}}_i^{\mathrm{T}}(k)\left(\boldsymbol{\Lambda}_S^{\mathrm{T}}\boldsymbol{P}\boldsymbol{\Lambda}_S-\boldsymbol{P}\right)\tilde{\boldsymbol{\eta}}_i(k)-2\tilde{\boldsymbol{\eta}}_i^{\mathrm{T}}(k)\boldsymbol{\Lambda}_S^{\mathrm{T}}\boldsymbol{P}\gamma_{\lambda_i}\boldsymbol{\Lambda}_{K_1U}\tilde{\boldsymbol{\eta}}_i(k-\tau_k)-\tilde{\boldsymbol{\eta}}_i^{\mathrm{T}}(k-\tau_k)\left(\gamma_{\lambda_i}\boldsymbol{\Lambda}_{K_1U}\right)^{\mathrm{T}}\boldsymbol{P}\gamma_{\lambda_i}\boldsymbol{\Lambda}_{K_1U}\tilde{\boldsymbol{\eta}}_i(k-\tau_k) \tag{19}$$

$$\Delta V_{i2}(k)\le\tilde{\boldsymbol{\eta}}_i^{\mathrm{T}}(k)\boldsymbol{Q}_1\tilde{\boldsymbol{\eta}}_i(k)-\tilde{\boldsymbol{\eta}}_i^{\mathrm{T}}(k-\tau_k)\boldsymbol{Q}_1\tilde{\boldsymbol{\eta}}_i(k-\tau_k)+\sum_{l=k+1-\tau_M}^{k-\tau_m}\tilde{\boldsymbol{\eta}}_i^{\mathrm{T}}(l)\boldsymbol{Q}_1\tilde{\boldsymbol{\eta}}_i(l) \tag{20}$$

$$\Delta V_{i3}(k)=\tilde{\boldsymbol{\eta}}_i^{\mathrm{T}}(k)\boldsymbol{Q}_2\tilde{\boldsymbol{\eta}}_i(k)-\tilde{\boldsymbol{\eta}}_i^{\mathrm{T}}(k-\tau_m)\boldsymbol{Q}_2\tilde{\boldsymbol{\eta}}_i(k-\tau_m)+\tilde{\boldsymbol{\eta}}_i^{\mathrm{T}}(k)\boldsymbol{Q}_3\tilde{\boldsymbol{\eta}}_i(k)-\tilde{\boldsymbol{\eta}}_i^{\mathrm{T}}(k-\tau_M)\boldsymbol{Q}_3\tilde{\boldsymbol{\eta}}_i(k-\tau_M) \tag{21}$$

$$\Delta V_{i4}(k)=\rho\tilde{\boldsymbol{\eta}}_i^{\mathrm{T}}(k)\boldsymbol{Q}_1\tilde{\boldsymbol{\eta}}_i(k)-\sum_{l=k+1-\tau_M}^{k-\tau_m}\tilde{\boldsymbol{\eta}}_i^{\mathrm{T}}(l)\boldsymbol{Q}_1\tilde{\boldsymbol{\eta}}_i(l) \tag{22}$$

$$\Delta V_{i5}(k)=\rho\boldsymbol{\upsilon}_i^{\mathrm{T}}(k)\boldsymbol{R}\boldsymbol{\upsilon}_i(k)-\sum_{l=k-\tau_M}^{k-\tau_m-1}\boldsymbol{\upsilon}_i^{\mathrm{T}}(l)\boldsymbol{R}\boldsymbol{\upsilon}_i(l) \tag{23}$$

$$\Delta V_{i6}(k)=\tau_M\boldsymbol{\upsilon}_i^{\mathrm{T}}(k)\boldsymbol{\Gamma}\boldsymbol{\upsilon}_i(k)-\sum_{l=k-\tau_M}^{k-1}\boldsymbol{\upsilon}_i^{\mathrm{T}}(l)\boldsymbol{\Gamma}\upsilon_i(l) \tag{24}$$

Because

$$-\sum_{l=k-\tau_M}^{k-\tau_m-1}\boldsymbol{\upsilon}_i^{\mathrm{T}}(l)\boldsymbol{R}\boldsymbol{\upsilon}_i(l)=-\sum_{l=k-\tau_M}^{k-\tau_k-1}\boldsymbol{\upsilon}_i^{\mathrm{T}}(l)\boldsymbol{R}\boldsymbol{\upsilon}_i(l)-\sum_{l=k-\tau_k}^{k-\tau_m-1}\boldsymbol{\upsilon}_i^{\mathrm{T}}(l)\boldsymbol{R}\boldsymbol{\upsilon}_i(l) \tag{25}$$

$$-\sum_{l=k-\tau_M}^{k-1}\boldsymbol{\upsilon}_i^{\mathrm{T}}(l)\boldsymbol{\Gamma}\boldsymbol{\upsilon}_i(l)=-\sum_{l=k-\tau_M}^{k-\tau_k-1}\boldsymbol{\upsilon}_i^{\mathrm{T}}(l)\boldsymbol{\Gamma}\boldsymbol{\upsilon}_i(l)-\sum_{l=k-\tau_k}^{k-1}\boldsymbol{\upsilon}_i^{\mathrm{T}}(l)\boldsymbol{\Gamma}\boldsymbol{\upsilon}_i(l) \tag{26}$$

Denote $\boldsymbol{\zeta}_i(k)=\left[\tilde{\boldsymbol{\eta}}_i^{\mathrm{T}}(k),\tilde{\boldsymbol{\eta}}_i^{\mathrm{T}}(k-\tau_k),\tilde{\boldsymbol{\eta}}_i^{\mathrm{T}}(k-\tau_m),\tilde{\boldsymbol{\eta}}_i^{\mathrm{T}}(k-\tau_M)\right]^{\mathrm{T}}$,

$\boldsymbol{D}=\left[\boldsymbol{D}_1^{\mathrm{T}}\quad \boldsymbol{D}_2^{\mathrm{T}}\quad \boldsymbol{0}\quad \boldsymbol{0}\right]^{\mathrm{T}}$, $\boldsymbol{T}=\left[\boldsymbol{T}_1^{\mathrm{T}}\quad \boldsymbol{T}_2^{\mathrm{T}}\quad \boldsymbol{0}\quad \boldsymbol{0}\right]^{\mathrm{T}}$,

$\boldsymbol{\Psi}=\left[\boldsymbol{\Psi}_1^{\mathrm{T}}\quad \boldsymbol{\Psi}_2^{\mathrm{T}}\quad \boldsymbol{0}\quad \boldsymbol{0}\right]^{\mathrm{T}}$. By using *Lemma 3*, then

$$\begin{aligned}
&-\sum_{l=k-\tau_k}^{k-1}\boldsymbol{\upsilon}_i^{\mathrm{T}}(l)\boldsymbol{\Gamma}\boldsymbol{\upsilon}_i(l)\le 2\sum_{l=k-\tau_k}^{k-1}\boldsymbol{\upsilon}_i^{\mathrm{T}}(l)\boldsymbol{\Psi}^{\mathrm{T}}\boldsymbol{\zeta}_i(k)+\\
&\sum_{l=k-\tau_k}^{k-1}\boldsymbol{\zeta}_i^{\mathrm{T}}(k)\boldsymbol{\Psi}\boldsymbol{\Gamma}^{-1}\boldsymbol{\Psi}^{\mathrm{T}}\boldsymbol{\zeta}_i(k)\\
&\le 2\tilde{\boldsymbol{\eta}}_i^{\mathrm{T}}(k)\boldsymbol{\Psi}_1^{\mathrm{T}}\tilde{\boldsymbol{\eta}}_i(k)+2\tilde{\boldsymbol{\eta}}_i^{\mathrm{T}}(k)\boldsymbol{\Psi}_2^{\mathrm{T}}\tilde{\boldsymbol{\eta}}_i(k-\tau_k)-\\
&2\tilde{\boldsymbol{\eta}}_i^{\mathrm{T}}(k-\tau_k)\boldsymbol{\Psi}_1^{\mathrm{T}}\tilde{\boldsymbol{\eta}}_i(k)-2\tilde{\boldsymbol{\eta}}_i^{\mathrm{T}}(k-\tau_k)\boldsymbol{\Psi}_2^{\mathrm{T}}\tilde{\boldsymbol{\eta}}_i(k-\tau_k)+\\
&\tau_M\boldsymbol{\zeta}_i^{\mathrm{T}}(k)\boldsymbol{\Psi}\boldsymbol{\Gamma}^{-1}\boldsymbol{\Psi}^{\mathrm{T}}\boldsymbol{\zeta}_i(k)
\end{aligned}\tag{27}$$

$$\begin{aligned}
&-\sum_{l=k-\tau_k}^{k-\tau_m-1}\boldsymbol{\upsilon}_i^{\mathrm{T}}(l)\boldsymbol{R}\boldsymbol{\upsilon}_i(l)\le 2\sum_{l=k-\tau_k}^{k-\tau_m-1}\boldsymbol{\upsilon}_i^{\mathrm{T}}(l)\boldsymbol{T}^{\mathrm{T}}\boldsymbol{\zeta}_i(k)+\\
&\sum_{l=k-\tau_k}^{k-\tau_m-1}\boldsymbol{\zeta}_i^{\mathrm{T}}(k)\boldsymbol{T}\boldsymbol{R}^{-1}\boldsymbol{T}^{\mathrm{T}}\boldsymbol{\zeta}_i(k)\\
&\le 2\tilde{\boldsymbol{\eta}}_i^{\mathrm{T}}(k-\tau_m)\boldsymbol{T}_1^{\mathrm{T}}\tilde{\boldsymbol{\eta}}_i(k)+2\tilde{\boldsymbol{\eta}}_i^{\mathrm{T}}(k-\tau_m)\boldsymbol{T}_2^{\mathrm{T}}\tilde{\boldsymbol{\eta}}_i(k-\tau_k)-\\
&2\tilde{\boldsymbol{\eta}}_i^{\mathrm{T}}(k-\tau_k)\boldsymbol{T}_1^{\mathrm{T}}\tilde{\boldsymbol{\eta}}_i(k)-2\tilde{\boldsymbol{\eta}}_i^{\mathrm{T}}(k-\tau_k)\boldsymbol{T}_2^{\mathrm{T}}\tilde{\boldsymbol{\eta}}_i(k-\tau_k)+\\
&\rho\boldsymbol{\zeta}_i^{\mathrm{T}}(k)\boldsymbol{T}\boldsymbol{R}^{-1}\boldsymbol{T}^{\mathrm{T}}\boldsymbol{\zeta}_i(k)
\end{aligned}\tag{28}$$

$$\begin{aligned}
&-\sum_{l=k-\tau_M}^{k-\tau_k-1}\boldsymbol{\upsilon}_i^{\mathrm{T}}(l)\boldsymbol{\Gamma}\boldsymbol{\upsilon}_i(l)-\sum_{l=k-\tau_M}^{k-\tau_k-1}\boldsymbol{\upsilon}_i^{\mathrm{T}}(l)\boldsymbol{R}\boldsymbol{\upsilon}_i(l)\le\\
&2\sum_{l=k-\tau_M}^{k-\tau_k-1}\boldsymbol{\upsilon}_i^{\mathrm{T}}(l)\boldsymbol{D}^{T}\boldsymbol{\zeta}(k)+\sum_{l=k-\tau_M}^{k-\tau_k-1}\boldsymbol{\zeta}_i^{\mathrm{T}}(k)\boldsymbol{D}\left(\boldsymbol{R}+\boldsymbol{\Gamma}\right)^{-1}\boldsymbol{D}^{\mathrm{T}}\boldsymbol{\zeta}_i(k)\\
&\le 2\tilde{\boldsymbol{\eta}}_i^{\mathrm{T}}(k-\tau_k)\boldsymbol{D}_1^{\mathrm{T}}\tilde{\boldsymbol{\eta}}_i(k)+2\tilde{\boldsymbol{\eta}}_i^{\mathrm{T}}(k-\tau_k)\boldsymbol{D}_2^{\mathrm{T}}\tilde{\boldsymbol{\eta}}_i(k-\tau_k)-\\
&2\tilde{\boldsymbol{\eta}}_i^{\mathrm{T}}(k-\tau_M)\boldsymbol{D}_1^{\mathrm{T}}\tilde{\boldsymbol{\eta}}_i(k)-2\tilde{\boldsymbol{\eta}}_i^{\mathrm{T}}(k-\tau_M)\boldsymbol{D}_2^{\mathrm{T}}\tilde{\boldsymbol{\eta}}_i(k-\tau_k)+\\
&\rho\boldsymbol{\zeta}_i^{\mathrm{T}}(k)\boldsymbol{D}\left(\boldsymbol{R}+\boldsymbol{\Gamma}\right)^{-1}\boldsymbol{D}^{\mathrm{T}}\boldsymbol{\zeta}_i(k)
\end{aligned}\tag{29}$$

Base on (18)~(29), then

$$\begin{aligned}
&\Delta V_i(k)\le\\
&\boldsymbol{\zeta}_i^{\mathrm{T}}(k)\left(\boldsymbol{\Omega}+\rho\boldsymbol{D}(\boldsymbol{R}+\boldsymbol{\Gamma})^{-1}\boldsymbol{D}^{\mathrm{T}}+\rho\boldsymbol{T}\boldsymbol{R}^{-1}\boldsymbol{T}^{\mathrm{T}}+\tau_M\boldsymbol{\Psi}\boldsymbol{\Gamma}^{-1}\boldsymbol{\Psi}^{\mathrm{T}}\right)\boldsymbol{\zeta}_i(k)
\end{aligned}\tag{30}$$

where $\boldsymbol{\Omega}=\begin{bmatrix}\boldsymbol{\Omega}_{11}&\boldsymbol{\Omega}_{12}&\boldsymbol{T}_1&-\boldsymbol{D}_1\\ *&\boldsymbol{\Omega}_{22}&\boldsymbol{T}_2&-\boldsymbol{D}_2\\ *&*&-\boldsymbol{Q}_2&\boldsymbol{0}\\ *&*&*&-\boldsymbol{Q}_3\end{bmatrix}$,

$$\begin{aligned}
\boldsymbol{\Omega}_{11}&=\boldsymbol{\Lambda}_S^{\mathrm{T}}\boldsymbol{P}\boldsymbol{\Lambda}_S-\boldsymbol{P}+(\rho+1)\boldsymbol{Q}_1+\boldsymbol{Q}_2+\boldsymbol{Q}_3+\boldsymbol{\Psi}_1+\boldsymbol{\Psi}_1^{\mathrm{T}}+\\
&\rho(\boldsymbol{\Lambda}_S-\boldsymbol{I})^{\mathrm{T}}\boldsymbol{R}(\boldsymbol{\Lambda}_S-\boldsymbol{I})+\tau_M(\boldsymbol{\Lambda}_S-\boldsymbol{I})^{\mathrm{T}}\boldsymbol{\Gamma}(\boldsymbol{\Lambda}_S-\boldsymbol{I}),\\
\boldsymbol{\Omega}_{12}&=-\boldsymbol{\Lambda}_S^{\mathrm{T}}\boldsymbol{P}\boldsymbol{\gamma}_{\lambda_i}\boldsymbol{\Lambda}_{K_1U}-\rho(\boldsymbol{\Lambda}_S-\boldsymbol{I})^{\mathrm{T}}\boldsymbol{R}\gamma_{\lambda_i}\boldsymbol{\Lambda}_{K_1U}+\boldsymbol{\Psi}_2^{\mathrm{T}}-\boldsymbol{\Psi}_1-\boldsymbol{T}_1-\\
&\tau_M(\boldsymbol{\Lambda}_S-\boldsymbol{I})^{\mathrm{T}}\boldsymbol{\Gamma}\gamma_{\lambda_i}\boldsymbol{\Lambda}_{K_1U}+\boldsymbol{D}_1,\\
\boldsymbol{\Omega}_{22}&=(\gamma_{\lambda_i}\boldsymbol{\Lambda}_{K_1U})^{\mathrm{T}}\boldsymbol{P}\boldsymbol{\gamma}_{\lambda_i}\boldsymbol{\Lambda}_{K_1U}-\boldsymbol{Q}_1+\rho(\gamma_{\lambda_i}\boldsymbol{\Lambda}_{K_1U})^{\mathrm{T}}\boldsymbol{R}\boldsymbol{\gamma}_{\lambda_i}\boldsymbol{\Lambda}_{K_1U}+\\
&\tau_M(\gamma_{\lambda_i}\boldsymbol{\Lambda}_{K_1U})^{\mathrm{T}}\boldsymbol{\Gamma}\boldsymbol{\gamma}_{\lambda_i}\boldsymbol{\Lambda}_{K_1U}-\boldsymbol{\Psi}_2-\boldsymbol{\Psi}_2^{\mathrm{T}}-\boldsymbol{T}_2-\boldsymbol{T}_2^{\mathrm{T}}+\boldsymbol{D}_2+\boldsymbol{D}_2^{\mathrm{T}}.
\end{aligned}$$

Applying Schur complement, based on *Lemma 4*, when formula (13) holds, then systems (17) are asymptotically stable, which means $\lim_{k\to\infty}\tilde{\boldsymbol{\xi}}(k)=\lim_{k\to\infty}(\hat{\boldsymbol{\xi}}(k)-(-\boldsymbol{L}_1^{-1}\boldsymbol{L}_2\otimes\boldsymbol{I}_q)\boldsymbol{x}_E(k))=\boldsymbol{0}$. According to Lemma 2, there exists $\lim_{k\to\infty}\left(\hat{\boldsymbol{\xi}}^{\bar{i}}(k)-\left(\boldsymbol{1}_{n_{\bar{i}}}/(N-M)\right)\otimes\sum_{j=M+1}^{N}\boldsymbol{x}_j(k)\right)=\boldsymbol{0}$. The proof is finished.

*Remark 3*: In distributed observers (8), the leaders' outputs are using to estimate the average of leaders' states. Compared with leaders' states, the outputs are easier to measure.

*Remark 4*: System (15) and system (16) may not be equivalent, but when system (16) is stable, system (15) is also asymptotically stable.

Based on the distributed observers (8), the TVOGFT protocol $\boldsymbol{u}_i^{\bar{i}}(k)$ for follower $i$ of group $\bar{i}$ is designed as follows

$$\boldsymbol{u}_i^{\bar{i}}(k)=\boldsymbol{K}_{2i}\boldsymbol{x}_i^{\bar{i}}(k)+\boldsymbol{K}_{3i}\left(\hat{\boldsymbol{\xi}}_i^{\bar{i}}(k)+\boldsymbol{h}_i^{\bar{i}}(k)\right)+\boldsymbol{r}_i^{\bar{i}}(k)(\bar{i}=1,2,\cdots,g)\tag{31}$$

where $\boldsymbol{K}_{2i}\in\mathbb{R}^{m_i\times n_i}$, $\boldsymbol{K}_{3i}\in\mathbb{R}^{m_i\times q}$ are constant matrices. $\boldsymbol{r}_i^{\bar{i}}(k)\in\mathbb{R}^{m_i}$ is the compensation input.

Because $rank(\boldsymbol{B}_i)=m_i$, there exists a nonsingular matrix $\Upsilon_i=\left[\hat{\boldsymbol{B}}_i^{\mathrm{T}},\tilde{\boldsymbol{B}}_i^{\mathrm{T}}\right]^{\mathrm{T}}$ satisfying $\hat{\boldsymbol{B}}_i\boldsymbol{B}_i=\boldsymbol{I}$, $\tilde{\boldsymbol{B}}_i\boldsymbol{B}_i=\boldsymbol{0}$, where $\hat{\boldsymbol{B}}_i\in\mathbb{R}^{m_i\times n_i}$, $\tilde{\boldsymbol{B}}_i\in\mathbb{R}^{(n_i-m_i)\times n_i}$. The Algorithm to construct the protocols (31) is given in the following.

*Algorithm 1*: the control input (31) for the follower $i$ of group $\bar{i}\,(\bar{i}=1,2,\cdots,g)$ can be constructed as below.

Step1: Solve regulation equation (3) for solution pairs $(\boldsymbol{E}_i,\boldsymbol{F}_i),i=1,2,\cdots,M$.

Step 2: For the given $\boldsymbol{h}_i^{\bar{i}}(k)$, verify the following equation

$$\tilde{\boldsymbol{B}}_i\boldsymbol{E}_i\left(\boldsymbol{S}\boldsymbol{h}_i^{\bar{i}}(k)-\boldsymbol{h}_i^{\bar{i}}(k+1)\right)=\boldsymbol{0}\tag{32}$$

If (32) holds, continue Step 3. Otherwise, the Algorithm stops.

Step3: Calculate $\boldsymbol{r}_i^{\bar{i}}(k)$ as

$$\boldsymbol{r}_i^{\bar{i}}(k)=-\hat{\boldsymbol{B}}_i\boldsymbol{E}_i\left(\boldsymbol{S}\boldsymbol{h}_i^{\bar{i}}(k)-\boldsymbol{h}_i^{\bar{i}}(k+1)\right)\tag{33}$$

Step 4: According to *Theorem 1*, determine the appropriate matrix $\boldsymbol{K}_1$ to make formula (13) hold.

Step5: Choose $\boldsymbol{K}_{2i}$ to make all the eigenvalues of $(\boldsymbol{A}_i+\boldsymbol{B}_i\boldsymbol{K}_{2i})$ are within the unit circle, $\boldsymbol{K}_{3i}=\boldsymbol{F}_i-\boldsymbol{K}_{2i}\boldsymbol{E}_i$.

*Remark 5*: In step 4 of *Algorithm 1*, the number of formula (13) for determining $\boldsymbol{K}_1$ is independent of the number of followers. In other steps, it is necessary to calculate the corresponding data for each follower, including $(\boldsymbol{E}_i, \boldsymbol{F}_i)$, $\tilde{\boldsymbol{B}}_i$, $\hat{\boldsymbol{B}}_i$, $\boldsymbol{r}_i^{\bar{i}}(k)$, $\boldsymbol{K}_{2i}$ and $\boldsymbol{K}_{3i} (i = 1, 2, \cdots, M)$, and the execution time will be extended with the increase of the number of followers.

Then *Theorem 2* is given to illustrate the effectiveness of protocols (31).

*Theorem 2*: Suppose *Assumptions 1~4* hold. When time-varying function $\boldsymbol{h}_i^{\bar{i}}(k)$ satisfies (32) and formula (13) holds, then the followers (1) can realize TVOGFT under the proposed protocols (31) with parameters determined in *Algorithm 1*.

*Proof*: The followers with protocols (31) can be written as

$$\boldsymbol{x}_i^{\bar{i}}(k+1) = \left(\boldsymbol{A}_i + \boldsymbol{B}_i \boldsymbol{K}_{2i}\right) \boldsymbol{x}_i^{\bar{i}}(k) + \boldsymbol{B}_i \boldsymbol{K}_{3i} \left(\hat{\boldsymbol{\xi}}_i^{\bar{i}}(k) + \boldsymbol{h}_i^{\bar{i}}(k)\right) + \boldsymbol{B}_i \boldsymbol{r}_i^{\bar{i}}(k), \bar{i} = 1, 2, \cdots, g \tag{34}$$

Denote $\xi(k) = \left(1/(N-M)\right) \sum_{j=M+1}^{N} \boldsymbol{x}_j(k)$, $\tilde{\boldsymbol{\xi}}_i^{\bar{i}}(k) = \hat{\boldsymbol{\xi}}_i^{\bar{i}}(k) - \xi(k)$, $\phi_i^{\bar{i}}(k) = \boldsymbol{x}_i^{\bar{i}}(k) - \boldsymbol{E}_i(\boldsymbol{h}_i^{\bar{i}}(k) + \xi(k))$.

Notice that $\xi(k+1) = \boldsymbol{S}\xi(k)$, then

$$\begin{aligned}\phi_i^{\bar{i}}(k+1) &= \left(\boldsymbol{A}_i + \boldsymbol{B}_i \boldsymbol{K}_{2i}\right) \phi_i^{\bar{i}}(k) + \boldsymbol{B}_i \boldsymbol{K}_{3i} \tilde{\boldsymbol{\xi}}_i^{\bar{i}}(k) + \boldsymbol{B}_i \boldsymbol{r}_i^{\bar{i}}(k) + \\ &\left(\boldsymbol{A}_i + \boldsymbol{B}_i \boldsymbol{K}_{2i}\right) \boldsymbol{E}_i \boldsymbol{h}_i^{\bar{i}}(k) + \boldsymbol{B}_i \boldsymbol{K}_{3i} \boldsymbol{h}_i^{\bar{i}}(k) - \boldsymbol{E}_i \boldsymbol{h}_i^{\bar{i}}(k+1) + \\ &\left(\boldsymbol{A}_i + \boldsymbol{B}_i \boldsymbol{K}_{2i}\right) \boldsymbol{E}_i \xi(k) + \boldsymbol{B}_i \boldsymbol{K}_{3i} \xi(k) - \boldsymbol{E}_i \boldsymbol{S} \xi(k)\end{aligned} \tag{35}$$

Choose $\boldsymbol{K}_{3i} = \boldsymbol{F}_i - \boldsymbol{K}_{2i} \boldsymbol{E}_i$, then (35) can be rewritten as

$$\phi_i^{\bar{i}}(k+1) = \left(\boldsymbol{A}_i + \boldsymbol{B}_i \boldsymbol{K}_{2i}\right) \phi_i^{\bar{i}}(k) + \boldsymbol{B}_i \boldsymbol{K}_{3i} \tilde{\boldsymbol{\xi}}_i^{\bar{i}}(k) + \boldsymbol{B}_i \boldsymbol{r}_i^{\bar{i}}(k) + \boldsymbol{E}_i \boldsymbol{S} \boldsymbol{h}_i^{\bar{i}}(k) - \boldsymbol{E}_i \boldsymbol{h}_i^{\bar{i}}(k+1) \tag{36}$$

When $\boldsymbol{h}_i^{\bar{i}}(k)$ satisfy (32), then

$$\tilde{\boldsymbol{B}}_i \boldsymbol{E}_i \left(\boldsymbol{S} \boldsymbol{h}_i^{\bar{i}}(k) - \boldsymbol{h}_i^{\bar{i}}(k+1)\right) + \tilde{\boldsymbol{B}}_i \boldsymbol{B}_i \boldsymbol{r}_i^{\bar{i}}(k) = \boldsymbol{0} \tag{37}$$

According to (33), then

$$\hat{\boldsymbol{B}}_i \boldsymbol{E}_i \left(\boldsymbol{S} \boldsymbol{h}_i^{\bar{i}}(k) - \boldsymbol{h}_i^{\bar{i}}(k+1)\right) + \hat{\boldsymbol{B}}_i \boldsymbol{B}_i \boldsymbol{r}_i^{\bar{i}}(k) = \boldsymbol{0} \tag{38}$$

Combining (37) and (38), since $\Upsilon_i = \left[\hat{\boldsymbol{B}}_i^{\mathrm{T}}, \tilde{\boldsymbol{B}}_i^{\mathrm{T}}\right]^{\mathrm{T}}$ is nonsingular, so

$$\phi_i^{\bar{i}}(k+1) = \left(\boldsymbol{A}_i + \boldsymbol{B}_i \boldsymbol{K}_{2i}\right) \phi_i^{\bar{i}}(k) + \boldsymbol{B}_i \boldsymbol{K}_{3i} \tilde{\boldsymbol{\xi}}_i^{\bar{i}}(k) \tag{39}$$

When formula (13) hold, then $\lim_{k\to\infty} \tilde{\boldsymbol{\xi}}_i^{\bar{i}}(k) = \boldsymbol{0}$. If choose $\boldsymbol{K}_{2i}$ to make all the eigenvalues of $\left(\boldsymbol{A}_i + \boldsymbol{B}_i \boldsymbol{K}_{2i}\right)$ are within the unit circle, then $\lim_{k\to\infty} \phi_i^{\bar{i}}(k) = \boldsymbol{0}$, which means

$$\lim_{k\to\infty} \left(\boldsymbol{x}_i^{\bar{i}}(k) - \boldsymbol{E}_i(\boldsymbol{h}_i^{\bar{i}}(k) + \xi(k))\right) = \boldsymbol{0} \tag{40}$$

Because $\boldsymbol{C}_i \boldsymbol{E}_i = \boldsymbol{U}$, so

$$\begin{aligned}&\lim_{k\to\infty} \left(\boldsymbol{C}_i \boldsymbol{x}_i^{\bar{i}}(k) - \boldsymbol{C}_i \boldsymbol{E}_i(\boldsymbol{h}_i^{\bar{i}}(k) + \xi(k))\right) = \\ &\lim_{k\to\infty} \left(\boldsymbol{y}_i^{\bar{i}}(k) - \boldsymbol{h}_{oi}^{\bar{i}}(k) - \frac{1}{N-M} \sum_{j=M+1}^{N} \boldsymbol{y}_j(k)\right) = \boldsymbol{0}\end{aligned} \tag{41}$$

which also indicates

$$\lim_{k\to\infty} \left(\boldsymbol{y}^{\bar{i}}(k) - \boldsymbol{h}_o^{\bar{i}}(k) - \left(\boldsymbol{1}_{n_{\bar{i}}} / (N-M)\right) \otimes \sum_{j=M+1}^{N} \boldsymbol{y}_j(k)\right) = \boldsymbol{0} \tag{42}$$

According to *Definition 1*, the control goal is achieved under the proposed protocols (31). The proof is finished.

## 4. NUMERICAL SIMULATION

In this section, a MAS consisted of ten followers (labeled 1~10) and three leaders (labeled 11~13) is considered, whose interactive topology is shown in Fig.1. The ten followers are divided into two groups, where followers 1~6 belong to group 1, and the others belong to group 2. The agent 2 and agent 7 are well-informed agents of each group which satisfy *Assumption 3*. Furthermore, group 2 can receive information of group1, and the interactive weight satisfies *Assumption 4*.

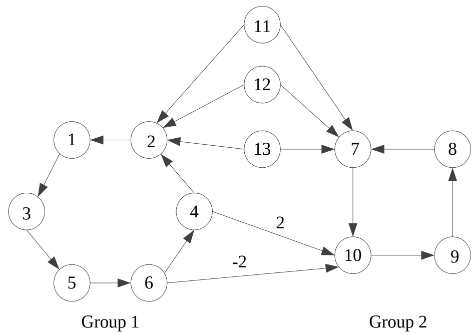


Fig.1. Interaction topology of MAS.

The parameters of three leaders are assumed to be $\boldsymbol{S} = \boldsymbol{I}_2 \otimes \begin{bmatrix} \cos T & \sin T \\ -1 & 1 \end{bmatrix}$, $\boldsymbol{U} = \boldsymbol{I}_2 \otimes \begin{bmatrix} 1 & 0 \end{bmatrix}$. Considering the heterogeneous dynamics of the followers with $\boldsymbol{A}_1 = \boldsymbol{A}_2 = \boldsymbol{I}_2 \otimes \begin{bmatrix} \cos T & \sin T \\ 0 & 0 \end{bmatrix}$, $\boldsymbol{B}_1 = \boldsymbol{B}_2 = \boldsymbol{I}_2 \otimes \begin{bmatrix} 0 \\ 1 \end{bmatrix}$, $\boldsymbol{C}_1 = \boldsymbol{C}_2 = \boldsymbol{I}_2 \otimes \begin{bmatrix} 1 & 0 \end{bmatrix}$, $\boldsymbol{A}_3 = \boldsymbol{A}_4 = \boldsymbol{I}_2 \otimes \begin{bmatrix} \cos T & \sin T & 0 \\ 0 & 0 & 1 \\ 0 & 1 & 0 \end{bmatrix}$, $\boldsymbol{B}_3 = \boldsymbol{B}_4 = \boldsymbol{I}_2 \otimes \begin{bmatrix} 0 & 0 \\ 0 & 1 \\ 1 & 0 \end{bmatrix}$, $\boldsymbol{C}_3 = \boldsymbol{C}_4 = \boldsymbol{I}_2 \otimes \begin{bmatrix} 1 & 0 & 0 \end{bmatrix}$, $\boldsymbol{A}_5 = \boldsymbol{A}_6 = \boldsymbol{I}_2 \otimes \begin{bmatrix} \cos T & \sin T & 0 \\ 0 & 0 & 1 \\ 0 & 1 & 0 \end{bmatrix}$, $\boldsymbol{B}_5 = \boldsymbol{B}_6 = \boldsymbol{I}_2 \otimes \begin{bmatrix} 0 & 0 \\ 1 & 0 \\ 0 & 1 \end{bmatrix}$, $\boldsymbol{C}_5 = \boldsymbol{C}_6 = \boldsymbol{I}_2 \otimes \begin{bmatrix} 1 & 0 & 0 \end{bmatrix}$, $\boldsymbol{A}_7 = \boldsymbol{A}_8 = \boldsymbol{I}_2 \otimes \begin{bmatrix} \cos T & \sin T \\ -3 & -1 \end{bmatrix}$,

$\boldsymbol{B}_7 = \boldsymbol{B}_8 = \boldsymbol{I}_2 \otimes \begin{bmatrix} 0 \\ 2 \end{bmatrix}$ , $\boldsymbol{C}_7 = \boldsymbol{C}_8 = \boldsymbol{I}_2 \otimes \begin{bmatrix} 1 & 0 \end{bmatrix}$ ,

$\boldsymbol{A}_9 = \boldsymbol{A}_{10} = \boldsymbol{I}_2 \otimes \begin{bmatrix} \cos T & \sin T & 0 \\ -1 & 2 & 1 \\ 0 & -1 & -1 \end{bmatrix}$, $\boldsymbol{B}_9 = \boldsymbol{B}_{10} = \boldsymbol{I}_2 \otimes \begin{bmatrix} 0 & 0 \\ 1 & 0 \\ 0 & 1 \end{bmatrix}$,

$\boldsymbol{C}_9 = \boldsymbol{C}_{10} = \boldsymbol{I}_2 \otimes \begin{bmatrix} 1 & 0 & 0 \end{bmatrix}$.

The followers in group 1 and group 2 are expected to form different formations, which are defined by the following time-varying formation functions

$$\boldsymbol{h}_i^1(k) = \begin{bmatrix} \cos(kT + \frac{i-1}{3}\pi) \\ -\sin(kT + \frac{i-1}{3}\pi) \\ \sin(kT + \frac{i-1}{3}\pi) \\ \cos(kT + \frac{i-1}{3}\pi) \end{bmatrix}, i = 1, 2, \cdots, 6,$$

$$\boldsymbol{h}_i^2(k) = 0.5 * \begin{bmatrix} \cos(kT + \frac{i-7}{2}\pi) \\ -\sin(kT + \frac{i-7}{2}\pi) \\ \sin(kT + \frac{i-7}{2}\pi) \\ \cos(kT + \frac{i-7}{2}\pi) \end{bmatrix}, i = 7, 8, 9, 10.$$

According to *Algorithm 1*, the pairs $(\boldsymbol{E}_i, \boldsymbol{F}_i)(i = 1, 2, \cdots, 10)$ are calculated by *Assumption 1* as $\boldsymbol{E}_1 = \boldsymbol{E}_2 = \boldsymbol{I}_2 \otimes \boldsymbol{I}_2$ ,

$\boldsymbol{F}_1 = \boldsymbol{F}_2 = \boldsymbol{I}_2 \otimes \begin{bmatrix} -1 & 1 \end{bmatrix}$ , $\boldsymbol{E}_3 = \boldsymbol{E}_4 = \boldsymbol{I}_2 \otimes \begin{bmatrix} 1 & 0 \\ 0 & 1 \\ 0 & 0 \end{bmatrix}$ ,

$\boldsymbol{F}_3 = \boldsymbol{F}_4 = \boldsymbol{I}_2 \otimes \begin{bmatrix} 0 & -1 \\ -1 & 1 \end{bmatrix}$ , $\boldsymbol{E}_5 = \boldsymbol{E}_6 = \boldsymbol{I}_2 \otimes \begin{bmatrix} 1 & 0 \\ 0 & 1 \\ 0 & 0 \end{bmatrix}$ ,

$\boldsymbol{F}_5 = \boldsymbol{F}_6 = \boldsymbol{I}_2 \otimes \begin{bmatrix} -1 & 1 \\ 0 & -1 \end{bmatrix}$ , $\boldsymbol{E}_7 = \boldsymbol{E}_8 = \boldsymbol{I}_2 \otimes \boldsymbol{I}_2$ ,

$\boldsymbol{F}_7 = \boldsymbol{F}_8 = \boldsymbol{I}_2 \otimes \begin{bmatrix} 1 & 1 \end{bmatrix}$ , $\boldsymbol{E}_9 = \boldsymbol{E}_{10} = \boldsymbol{I}_2 \otimes \begin{bmatrix} 1 & 0 \\ 0 & 1 \\ 0 & 0 \end{bmatrix}$ ,

$\boldsymbol{F}_9 = \boldsymbol{F}_{10} = \boldsymbol{I}_2 \otimes \begin{bmatrix} 0 & -1 \\ -1 & 1 \end{bmatrix}$.

By choosing matrices $\tilde{\boldsymbol{B}}_1 = \tilde{\boldsymbol{B}}_2 = \boldsymbol{I}_2 \otimes \begin{bmatrix} 1 & 0 \end{bmatrix}$ , $\hat{\boldsymbol{B}}_1 = \hat{\boldsymbol{B}}_2 = \boldsymbol{I}_2 \otimes \begin{bmatrix} 0 & 1 \end{bmatrix}$ , $\tilde{\boldsymbol{B}}_3 = \tilde{\boldsymbol{B}}_4 = \boldsymbol{I}_2 \otimes \begin{bmatrix} 1 & 0 & 0 \end{bmatrix}$ , $\hat{\boldsymbol{B}}_3 = \hat{\boldsymbol{B}}_4 = \boldsymbol{I}_2 \otimes \begin{bmatrix} 0 & 0 & 1 \\ 0 & 1 & 0 \end{bmatrix}$ , $\tilde{\boldsymbol{B}}_5 = \tilde{\boldsymbol{B}}_6 = \boldsymbol{I}_2 \otimes \begin{bmatrix} 1 & 0 & 0 \end{bmatrix}$ , $\hat{\boldsymbol{B}}_5 = \hat{\boldsymbol{B}}_6 = \boldsymbol{I}_2 \otimes \begin{bmatrix} 0 & 1 & 0 \\ 0 & 0 & 1 \end{bmatrix}$ , $\tilde{\boldsymbol{B}}_7 = \tilde{\boldsymbol{B}}_8 = \boldsymbol{I}_2 \otimes \begin{bmatrix} 1 & 0 \end{bmatrix}$ , $\hat{\boldsymbol{B}}_7 = \hat{\boldsymbol{B}}_8 = \boldsymbol{I}_2 \otimes \begin{bmatrix} 0 & 0.5 \end{bmatrix}$ , $\tilde{\boldsymbol{B}}_9 = \tilde{\boldsymbol{B}}_{10} = \boldsymbol{I}_2 \otimes \begin{bmatrix} 1 & 0 & 0 \end{bmatrix}$ , $\hat{\boldsymbol{B}}_9 = \hat{\boldsymbol{B}}_{10} = \boldsymbol{I}_2 \otimes \begin{bmatrix} 0 & 1 & 0 \\ 0 & 0 & 1 \end{bmatrix}$ , it can be illustrated that $\boldsymbol{h}_i^{\bar{i}}(k)(\bar{i} = 1, 2)$ satisfy (32) for each follower. Then the compensation input $\boldsymbol{r}_i^{\bar{i}}(k)$ can be calculated according to formula (33) in *Algorithm 1*.

In step 4 of *Algorithm 1*, on the basis of *Theorem 1*, when $\boldsymbol{K}_1 = \boldsymbol{I}_2 \otimes \begin{bmatrix} 0.1 \\ 0.3 \end{bmatrix}$, formula (13) hold, and the error system(14) is asymptotically stable. The observer errors of ten followers belonged to group 1 and group 2 are shown in Fig.2 and Fig.3, respectively. The observer errors in the two figures asymptotically approach zero, which means $\lim_{k\to\infty}\left(\hat{\boldsymbol{\xi}}^{\bar{i}}(k) - \left(\boldsymbol{1}_{n_{\bar{i}}} / (N-M)\right) \otimes \sum_{j=M+1}^{N} \boldsymbol{x}_j(k)\right) = \boldsymbol{0}\left(\bar{i} = 1, 2\right)$ and indicate the observers (8) are effective to estimate the average of leaders' states.

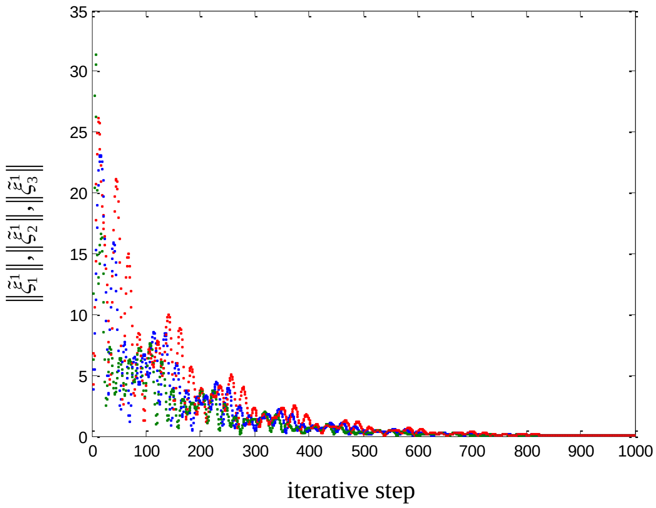


(a) Agents 1~3

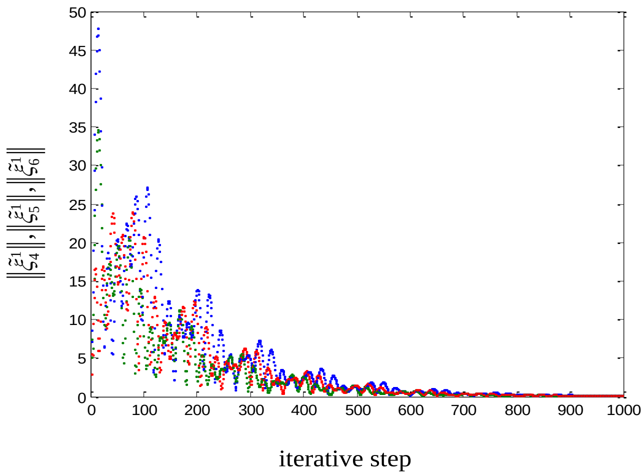


(b) Agents 4~6

Fig.2. Observer errors of group 1.

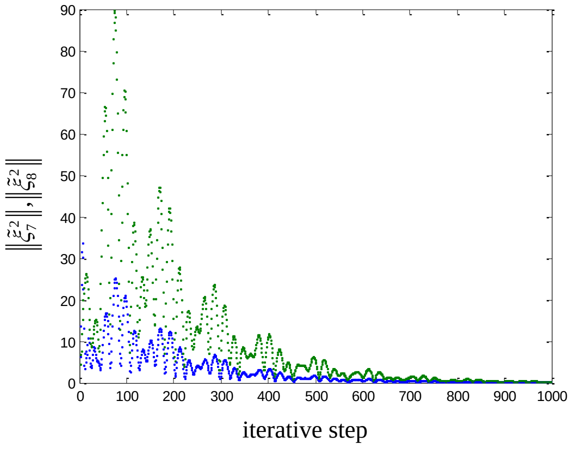


(a) Agents 7~8

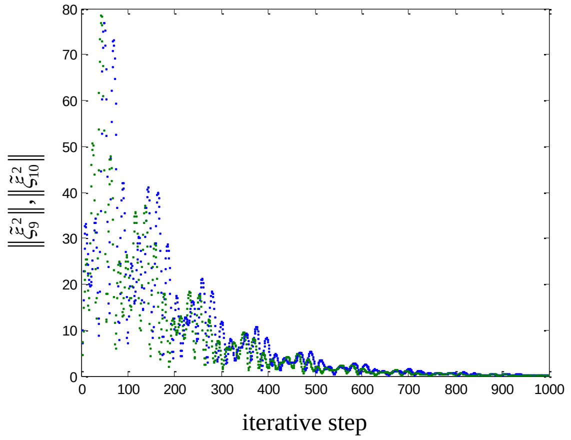


(b) Agents 9~10

Fig.3. Observer errors of group 2.

According to Step 5 of *Algorithm 1*, the matrices $\boldsymbol{K}_{2i}(i=1,2,\cdots,10)$ are chosen as

$$\boldsymbol{K}_{21}=\boldsymbol{K}_{22}=\boldsymbol{I}_2\otimes\begin{bmatrix}-2 & 0.01\end{bmatrix},$$

$$\boldsymbol{K}_{23}=\boldsymbol{K}_{24}=\boldsymbol{I}_2\otimes\begin{bmatrix}-2 & -0.1 & 0\\ 0 & -0.1 & -0.1\end{bmatrix},$$

$$\boldsymbol{K}_{25}=\boldsymbol{K}_{26}=\boldsymbol{I}_2\otimes\begin{bmatrix}0 & -0.1 & -0.1\\ -2 & -0.1 & 0\end{bmatrix},$$

$$\boldsymbol{K}_{27}=\boldsymbol{K}_{28}=\boldsymbol{I}_2\otimes\begin{bmatrix}-2 & 0.01\end{bmatrix},$$

$$\boldsymbol{K}_{29}=\boldsymbol{K}_{210}=\boldsymbol{I}_2\otimes\begin{bmatrix}0 & -1 & 0.01\\ 0 & -0.1 & 0\end{bmatrix},$$

and $\boldsymbol{K}_{3i}$ are determined by $\boldsymbol{K}_{3i}=\boldsymbol{F}_i-\boldsymbol{K}_{2i}\boldsymbol{E}_i(i=1,2,\cdots,10)$. Then control protocols (31) can be constructed.

After applying control protocols (31) to ten followers described as formula (1), the time-varying outputs snap shots at time instants $k=500,600,900,1000$ are shown in Fig.4, respectively, where the six followers of group 1 and four followers of group 2 rotate anticlockwise around the average of leaders' outputs, which is labeled by red lower triangle. Then the followers are said to form time-varying output group formation and track the average of leaders' outputs. It should be noticed that the Fig.1 only shows the network topology relationship between followers, while the followers' actual locations are determined by the formation functions.

In order to show that followers can track the average of leaders' outputs clearly, the tracking trajectories of followers of group 1 and group 2 are displayed in Fig.5 and Fig.6 respectively, where the average trajectory of leaders' outputs is labeled by blue line. It can be seen that the followers of group 1 and group 2 track the average of leaders' outputs while maintain the desired time-varying formation. For the sake of simplicity, only the agent 1 and agent 7 are marked in Fig.5 and Fig. 6, and the other agents are arranged in anticlockwise order, which is the same as in Fig. 4.

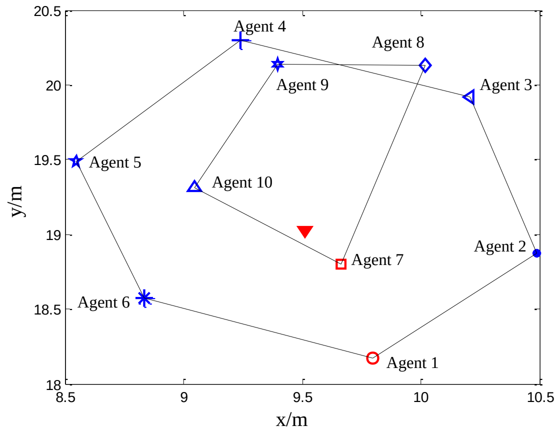


(a) $k=500$

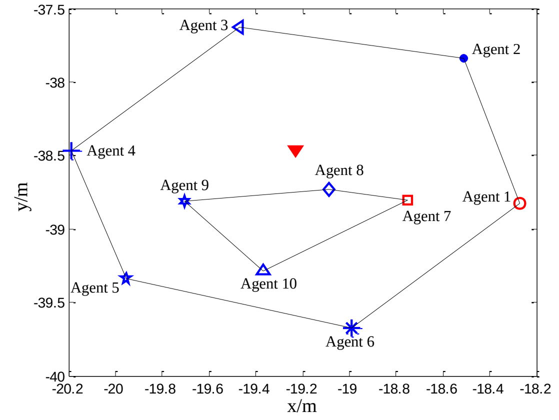


(b) $k=600$

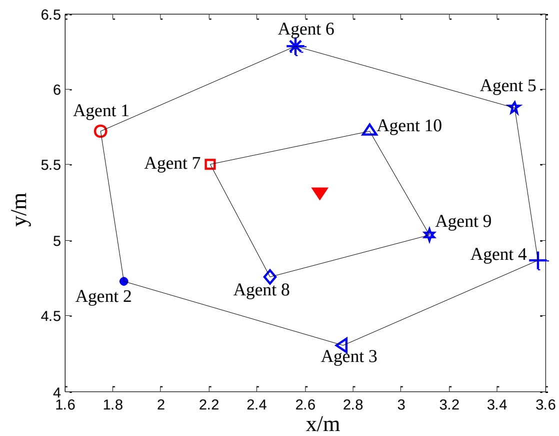


(c) $k=900$

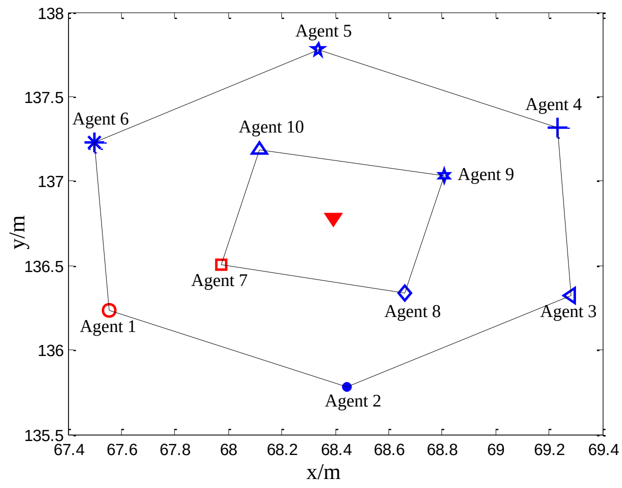


(d) $k=1000$

Fig.4. Time-varying outputs snap shots of followers.

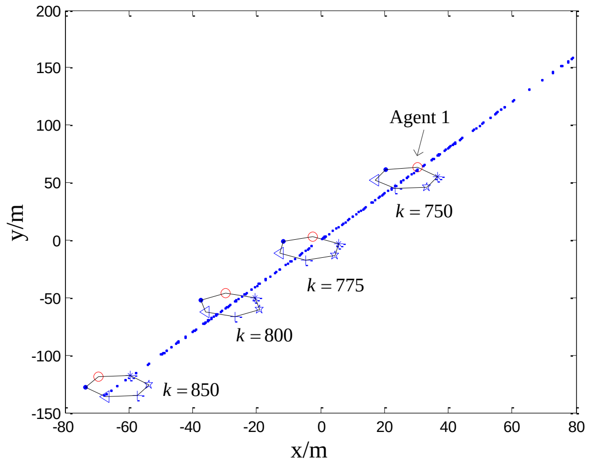


Fig.5. Tracking trajectories of followers of group 1.

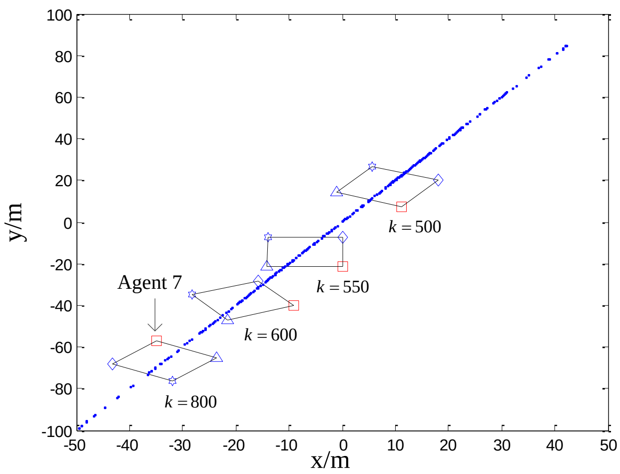


Fig.6.Tracking trajectories of followers of group 2.

To further demonstrate the effectiveness of proposed protocols, the formation tracking errors of followers $\phi_i^{\bar{i}}(k)\left(i=1,2,\cdots,10\right)$ in group 1 and group 2 are shown in Fig.7 and Fig.8, respectively. All the formation tracking errors of followers finally reach zero, and indicate the followers can realize the TVOGFT under control protocols with zero error according to Theorem 2.

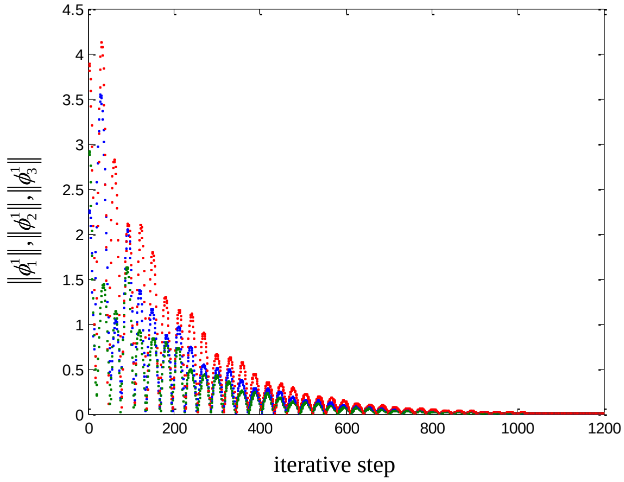


(a) Agents 1~3

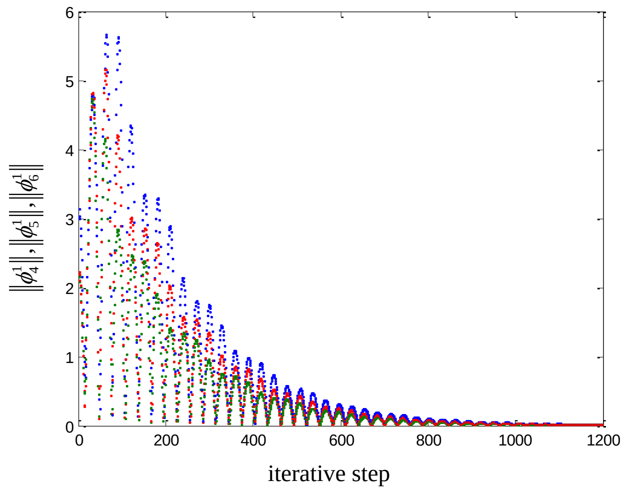


(b) Agents 4~6

Fig. 7. Formation tracking errors of group 1.

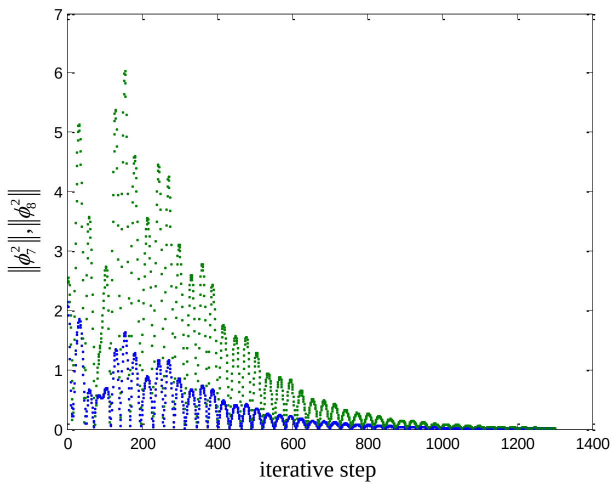


(a) Agents 7~8

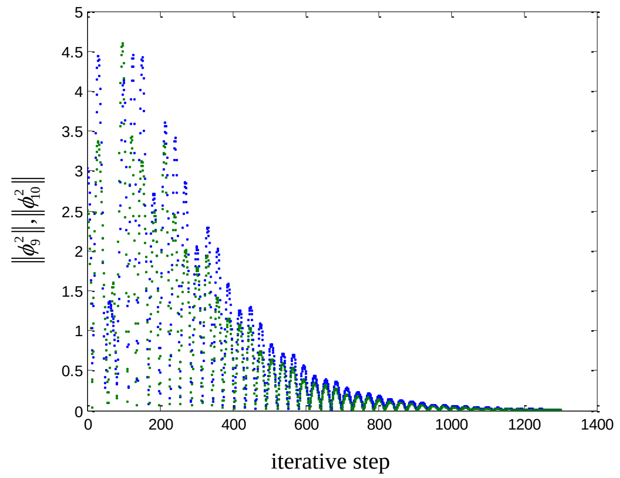


(b) Agents 9~10

Fig. 8. Formation tracking errors of group 2.

## 5. CONCLUSIONS

For the high-order discrete-time heterogeneous MAS consisted of multiple followers and leaders, the TVOGFT problem with time-varying communication delay is investigated in this paper. The observers to estimate the average of leaders' states are proposed by using neighboring outputs, whose effectiveness are proved based on Lyapunov theory. Then, the observer-based control protocols enabling followers to realize TVOGFT and Algorithm regulating the protocols are presented. The future work will focus on the group formation-containment tracking control of discrete-time heterogeneous MAS, in which all agents, including virtual leader, formation leaders and containment followers, have different dynamics.

## ACKNOWLEDGEMENTS

This work is supported by Science and Technology Program of Gansu Province under Grant 21JR7RM192, Gansu University Innovation Fund Project under Grant 2021B-260, Science and Technology Program of Gansu Province under Grants 21JR1RM339, 21JR11RM046.

## REFERENCES

Chen, Y.G., and Li, W.L.(2009). Improved results on robust $H_\infty$ control of uncertain discrete-time systems with time-varying delay. *International Journal of Automation and Computing*, 06(1), 103-108.

Dong, X.W., Li, Y.F., and Lu, C.(2019). Time-varying formation tracking for UAV swarm systems with switching directed topologies. *IEEE Transactions on Neural Networks and Learning Systems*, 30(13), 3674-3685.

Dong, X.W., and Hu, G.Q.(2016). Time-varying formation control for general linear multi-agent systems with switching directed topologies. *Automatica*, 73, 47-55.

Dong, X.W., Li, Q.D., and Zhao, Q.L.(2017). Time-varying group formation analysis and design for general linear multi-agent systems with directed topologies. *International Journal of Robust and Nonlinear Control*, 27(9), 1640-1652.

Duan, J., Zhang, H.G., and Cai, Y.L.(2020). Finite-time time-varying output formation-tracking of heterogeneous linear multi-agent systems. *Journal of the Franklin Institute*, 357, 926-941.

Gao, Z.Y., Zhang, H.G., and Wang, Y.C.(2021). Time-varying output formation-containment control for homogeneous/heterogeneous descriptor fractional-order multi-agent systems. *Information Science*, 567, 146-166.

Godsil, C., Royle, G.(2001). *Algebraic Graph Theory*. Springer, New York.

Gong, Y.F., Wen, G.G., and Peng, Z.X.(2020). Observer-based time-varying formation control of fractional-order multi-agent systems with general linear dynamics. *IEEE Transactions on Circuits and Systems*, 67, 82-86.

Guo, J., Yan, G.F., and Lin, Z.Y.(2010). Local control strategy for moving-target-enclosing under dynamically changing network topology. *System & Control Letters*, 59 (10), 654-661.

Han, L., Xie, Y.X., and Li, X.D.(2020). Time-varying group formation tracking control for second-order multi-agent systems with communication delays and multiple leaders. *Journal of Franklin Institute*, 357, 9761-9780.

Hu, J., Bhowmick, P., and Lanzon, A.(2019). Distributed adaptive time-varying group formation tracking for multiagent systems with multiple leaders on directed graphs, *IEEE Transactions on Control of Network Systems*, 7 (1), 140-150.

Hua, Y.Z., Dong, X.W., and Hu G.Q.(2019). Distributed time-varying output formation tracking for heterogeneous linear multi-agent systems with a nonautonomous leader of unknown input. *IEEE Transactions on Automatic Control*, 64(10), 4292-4299.

Hua, Y.Z., Dong, X.W., and Li Q.D.(2018). Fault-tolerant time-varying formation tracking for second-order multi-agent systems with actuator faults and a non-cooperative target. *IFAC* paper-online, 51(24), 68-73.

Hua, Y.Z., Dong, X.W., and Li, Q.D.(2020). Distributed adaptive formation tracking for heterogeneous multi-agent systems with multiple nonidentical leaders and without well-informed follower. *International journal of Robust Nonlinear Control*, 30, 2131-2151.

Hua, Y.Z., Dong, X.W., and Wang, J.B.(2019). Time-varying output formation tracking of heterogeneous linear multi-agent systems with multiple leaders and switching topologies. *Journal of the Franklin Institute*, 356, 539-560.

Jiang, W., Wang, C.Y., and Meng Y.H.(2020). Fully distributed time-varying formation tracking control of linear multi-agent systems with input delay and disturbances. *System& Control Letters*, 146, 104814.

Li, X.D., Bai, Y.M., and Dong, X.W.(2021). Distributed time-varying formation control with uncertainties based on an event-triggered mechanism. *Science China Information Science*, 64(3), 132204.

Li, X.D., Dong, X.W., and Li, Q.D.(2019). Event-triggered time-varying formation control for general linear multi-agent systems. *Journal of Franklin Institute*, 356(17), 10179-10195.

Li, Y.F., Dong, X.W., and Li, Q.D.(2018). Time-varying group formation tracking for second-order multi-agent systems with switching directed topologies. *IEEE CSAA Guidance, Navigation and Control Conference.IEEE*, 1-7.

Li, Z.K., Wen, G.H., and Duan, Z.S.(2015). Designing fully distributed consensus protocols for linear multi-agent systems with directed graphs. *IEEE Transaction on Automatic Control*, 60(4), 1152-1157.

Liu, C.Y., Wu, X.Q., and Wan, X.X.(2021).Time-varying output formation tracking of heterogeneous multi-agent systems with dynamical controllers. *Neurocomputing*, 441, 36-43.

Mahmoud M.S.(2004). *Resilient control of uncertain dynamical systems*. Springer-verlag, Berlin.

Maza, I., Kondak, K., and Bernard M.(2010). Multi-UAV cooperation and control for load transportation and deployment. *Journal of Intelligent and Robotic System,* 57, 417-449.

Qaisar, I., Aslam, S.M., and Zhou, C.(2020). Event-triggered based $H_\infty$ consensus control for multi-agent systems under time-varying delay. *Journal of Control Engineering and Applied Informatics*, 22 (3), 25-32.

Qi, X.L., and Yang, X.G.(2022). Time-varying output formation tracking control of discrete-time heterogeneous multi-agent systems. *Journal of System Simulation*, 34(1), 36-44.

Tian, L., Zhao, Q.L., Dong, X.W.(2020). Time-varying output group formation tracking for heterogeneous multi-agent systems. *Acta Aeronautica et Astronautica Sinica*, 41(7), 301-312.

Wang, J.H., Han L., and Li, X.D.(2020). Time-varying formation of second-order discrete-time multi-agent systems under nonuniform communication delays and switching topology with application to UAV formation flying. *IET Control Theory and Application*, 14(14), 1947-1956.

Wang, L., Xi, J.X., and He, M.(2020). Robust time-varying formation design for multi-agent systems with disturbances: extended-state-observer method. *International Journal of Robust and Nonlinear Control*, 30(7), 2796-280.

Wang, M., and Zhang, T.(2021). Leader-following formation control of second-order nonlinear systems with time-varying communication delay. *International Journal of Control, Automation and Systems*, 19(5), 1729-1739.

Wang, R., Dong, X.W., and Li Q.D.(2019). Distributed time-varying formation control for linear swarm systems with switching topologies using an adaptive output-feedback approach. *IEEE Transactions on Systems, Man, and Cybernetics: Systems*, 49(12), 2664-2675.

Wang, R., Dong, X.W., and Li Q.D.(2019). Distributed time-varying formation control for multiagent systems with directed topology using an adaptive output-feedback approach. *IEEE Transactions on Industrial Informatics*, 15(8), 4676- 4685.

Xi, J.X., Shi, Z.Y., and Zhong, Y.S.(2001). Consensus analysis and design for high-order linear swarm systems with time-varying delays. *Physica A*, 390(23-24), 4114-4123.

Yu, J.L., Dong, X.W., and Han, Liang(2020). Practical time-varying output formation tracking for high-order nonlinear strict-feedback multi-agent systems with input saturation. *ISA Transactions*, 98, 63-74.

Yu, J.L., Dong, X.W., and Li, Q.D.(2021). Distributed adaptive cooperative time-varying formation tracking guidance for multiple aerial vehicles system. *Aerospace Science and Technology*, 117, 106925.

Yu, J.L., Dong, X.W., and Li, Q.D.(2020). Robust $H_\infty$ guaranteed cost time-varying formation tracking for high-order multiagent systems with time-varying delays. *IEEE Transactions on Systems, Man, and Cybernetics: Systems*, 50(4), 1465-1475.

Zhang, B.Y., Xu, S.Y., and Zou, Y.(2008). Improved stability criterion and its application in delayed controller design for discrete-time systems. *Automatica*, 44(11), 2963-2967.

Zhou, S.Y., Wei, X.B., and Dong, X.W.(2021). Time-varying group formation-tracking control for heterogeneous multi-agent systems with switching topologies and time-varying delays. *Proceeding of the 40th Chinese control conference*. *IEEE*, 194-199.

Zuo, S., Song, Y.D., and Frank, L.L.(2019). Time-varying output formation containment of general linear homogeneous and heterogeneous multiagent systems. *IEEE Transactions on Control Network Systems*, 8(2), 537-548.

Zuo, X.(2021). A deep reinforcement learning methods based on deterministic policy gradient for multi-agent cooperative competition. *Journal of Control Engineering and Applied Informatics*, 23 (3), 88-98.